Seismic Lithofacies Classification over Turbidite Reservoir Offshore Brazil

Ricardo Luiz Bogado Duarte, Ricardo de Campos, Jose Fernando Rosalba, Marcelo Durval, Carlos Eduardo Abreu, PETROBRAS, Brazil
*Julio Tavares, Jean-Luc Formento, CGGVeritas, Brazil

Abstract

An integrated workflow, including careful seismic data preconditioning, simultaneous elastic inversion and seismic lithology classification has been applied to predict the distribution of five lithofacies in a complex turbiditic reservoir offshore Brazil. Four partial angle stacks (2°-40°) with 6 key wells, have been used to derive elastic properties through inversion. A well-based feasibility study shows that reservoir facies can be identified from a *Vp*/*Vs* ratio versus P-wave impedance (*Ip*) cross-plot. The main challenge for this seismic lithology discrimination was the complexity of the depositional system, which was tackled by incorporating a 3-D facies trend model in the seismic lithology prediction workflow. By applying a supervised Bayesian classification technique to our simultaneous elastic inversion results, litho-probability cubes were calculated for a total of 5 reservoir and non-reservoir facies. The inversion was performed in a layered stratigraphic framework constructed from interpreted horizons. This has yielded 3-D images of reservoir elastic properties and facies that better conform to the complex shapes of the channelized deposits.

Introduction

This paper presents the results of a 3-D simultaneous elastic inversion and a lithofacies classification over a Brazilian offshore field (~416 km^2). The target was the Miocene sequence, with two main reservoirs producing 70000 bbl/day, each one with a 25 to 30m average sand isopach, within a tectono-sedimentary depositional context. There are three eletrofacies corresponding to the following lithofacies: high permeability sandstones representing the system channel depositional axes, interlaminated sandstone and shale corresponding to the main system´s inter-channel heterogeneities and shale as non reservoir facies. The seismic response to lithology and fluid led to the definition of five seismic lithofacies in both reservoirs: shale, shaly sandstone with oil, oil sand, gas sand and water sand.

This work integrated data from 12 wells with lithofacies logs, of which only six have real S-wave logs. To build the stratigraphic model for the seismic inversion and lithofacies classification, eight main horizons, representing top and base of the units, were used. Four high density 3-D migrated seismic angle-stacks (bin 6.25m * 12.5m) and one seismic velocity volume were considered for this study. The main steps and challenges are described in the following sections.

Seismic Data Preconditioning

Analysis of the seismic energy over some key wells shows a strong E-W lateral variation, as observed in **Figure 1a**. To create a realistic RMS amplitude map, covering the reservoir intervals, two ghost horizons were created by shifting the top horizon of the first reservoir up by 400ms and down by 1100ms. The ghost horizons define a 1.5sec time window suitable for estimating the signal energy around the reservoirs. To compensate for the lateral variation in seismic energy, an amplitude correction map (see **Figure 1b**) was extracted across the selected time window and applied to the four angle stacks.

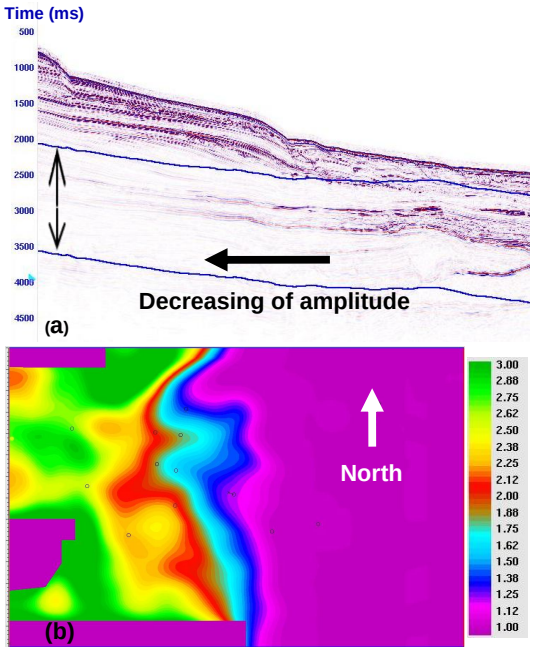

Figure 1: *(a) Section showing the time window used to compute the RMS amplitude map. (b) Amplitude correction map applied to all angle stacks.*

Figure 2 shows the impact of this correction on maps and sections.

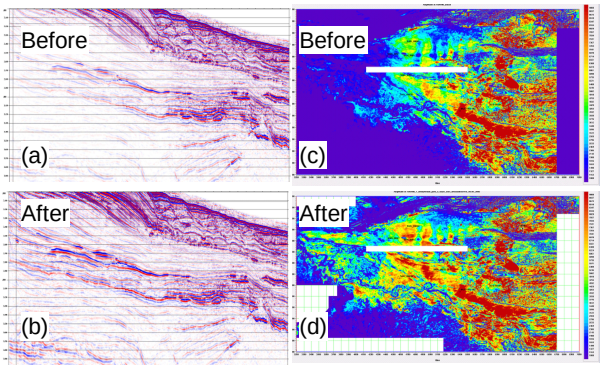

Figure 2: *Seismic section before (a) and after (b) amplitude correction, and horizon slice at the base of the reservoir before (c) and after (d)correction.*

By comparing the energy of the synthetic seismogram with the seismic trace of each angle stack, the computed Scaling Factor (SF), obtained from the seismic wavelet matching, gives a good estimation of the seismic amplitude variation. A scaling factor close to 1 at the different wells should be achieved prior to inversion for wavelet stationary. **Figure 3** shows the results of the wavelet extraction with the SF calculated before and after correction. This quality control (QC) gives confidence on the lateral amplitude correction applied to the different angle stacks. The correction was important to ensure the quality of the seismic inversion and of the inverted elastic properties used as the main input for the Bayesian lithofacies classification.

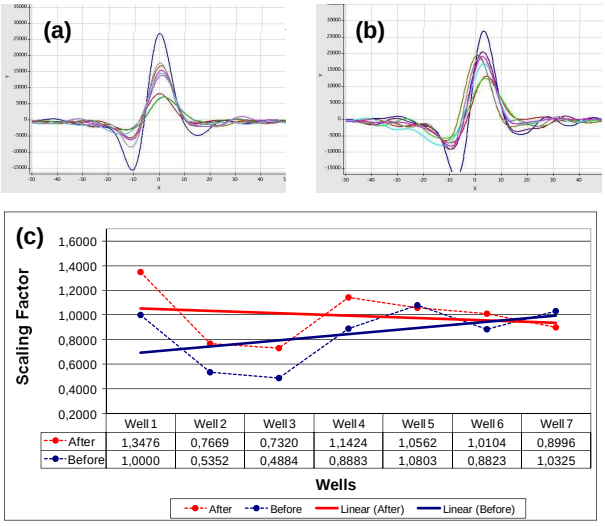

Figure 3: *Comparison between the wavelets and SF for each well. Extracted wavelets before (a) and after (b) the amplitude correction. Comparison (c) between the SF, for each well, before (blue) and after the correction (red). After correction, the SF values are around 1.*

A study of the time misalignment (DT) between angle stacks was also a key data conditioning step before inversion; poor data alignment leads to erroneous estimation of the AVO gradient and adversely affects the estimation of *Vp*/*Vs*. Time misalignment corrections were therefore applied prior to inversion to compensate residual NMO errors between the input angle stacks. These time corrections were computed by amplitude cross-correlation between consecutive angle stacks.

Lithofacies Analysis from Well Logs

From the 12 wells with digital logs, only 6 wells had real S-wave (*Vs*) logs. For the other wells, pseudo *Vs* were predicted using Castagna approach (Castagna et al., 1985). The synthetic *Vs* logs were only used to construct the low frequency initial model for the inversion, but were not considered for the inversion QC. Elastic attributes like P-Impedance (*Ip*), S-Impedance (*Is*), *Vp/Vs* ratio and the difference "*Ip-Is*" were derived for all wells from the *Vp, Vs* and density logs.

To create the training set for the lithofacies classification, fluid substitution was applied at the wells that had real *Vs* to create two extra facies: water sand and gas sand. The objective of fluid substitution was to model the elastic properties of the reservoir at the expected reservoir conditions (e.g., pressure, temperature, porosity, mineral type, and water salinity) and pore fluid saturation. Using the original well logs and the elastic values derived from the fluid substitution, several cross plots were analyzed to define the optimum combination of elastic attributes for discriminating the different lithofacies. **Figure 4** gives an explanation about the fluid substitution applied in the oil sand reservoirs only to create the two extra facies. Finally, five lithofacies were used in this project: shale, shaly sandstone with oil, oil sand, gas sand and water sand.

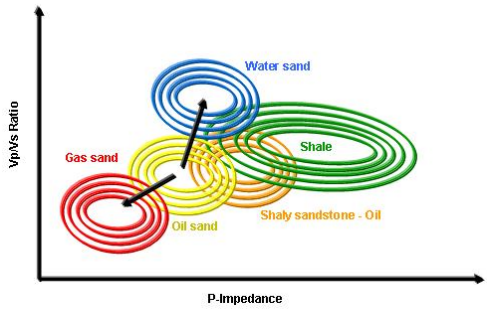

Figure 4: *Crossplot selected for the lithofacies classification and scheme of the fluid substitution.*

Stratigraphic Elastic Inversion

Eight horizons were provided by Petrobras to build the initial model; they were smoothed and edited to eliminate horizon crossing zones. The top of inversion window was created from a ghost horizon by shifting up the top first reservoir horizon by 200 ms. Top and base horizons from the two main reservoirs were used for the model layering. The base of the initial model was a geologic marker called Marco Azul.

The 3-D, multi-cube simultaneous inversion scheme starts from the initial layered elastic model defined in the time domain. During inversion, the initial model is interactively perturbed using a simulated annealing procedure to find a global solution that optimizes simultaneously the match between the four input angle stacks and the corresponding synthetics, calculated by convolution with full Zoeppritz reflectivity equations. In addition to a data mismatch term, the objective function contains 3-D spatial continuity constraints that are used to attenuate the effects of random noise. The inversion works by perturbing *Vp*, *Vs* and density in each cell of the 3-D stratigraphic grid. During inversion, independent perturbations of the different elastic parameters can be applied or perturbations can be coupled via correlations between *Vp*, *Vs* and density. In addition to updating the elastic parameters, the time-thickness of the micro-layers is also adjusted during the inversion process in order to maximize the coherence between the observed seismic events and the inversion layer framework.

Figure 5 shows the inversion results extracted at the one key well location, together with seismic traces and residuals. Comparison of the smooth initial model, the real blocky well log with the blocky inversion results demonstrates that the inversion yielded excellent estimates of the *Vp*/*Vs* ratio with a good decoupling between *Ip* and *Is*.

Lithofacies Classification

Following the inversion process, a Bayesian classification technique was applied to predict lithofacies from the inverted seismic data. Figure 6 illustrates the classification workflow. The log data (or pseudo-logs obtained by fluid substitution) are used to define a training set for each of the lithofacies that must be predicted. Cross plot of elastic attributes are created from the data points in the training set. The cross plot points are colour-coded according to lithofacies to assess visually the separability of the different lithologies. Next, a bivariate Probability Distribution Function (PDF) is fitted to each cluster of points using a non-parametric modeling technique. This conditional PDF is denoted by *f(z|c)* where *z* represents the elastic attribute vector (e.g., *Ip* and *Vp/Vs*) and *c* the lithofacies. After the training phase, the classifier is applied sample-by-sample to the input cubes of inverted elastic attributes: the likelihood of each lithofacies given the inverted attributes *z*, is calculated at each sample location from the computed bivariate PDFs. The procedure outputs likelihood cubes for the different lithofacies which can be used for uncertainty assessment. The most likely lithofacies, i.e., the facies *c* that maximizes *f(z|c)* is also calculated at each sample point. The maximum likelihood classification technique assumes implicitly that the occurrence of the different facies is a priori the same. In practice, geological information is often available about the facies proportions (e.g., information about net-to-gross ratio in the reservoir). This information can be incorporated using a priori facies proportions, *p(c)*. To combine the a priori information with the seismic-derived facies information, a posterior probability is computed for each lithofacies by multiplying the prior probability by the corresponding seismic likelihood, i.e., $p(c|z) \alpha f(z|c)p(c)$. Using this simple Bayesian updating rule, posterior probability cubes are computed for the different facies. The most probable facies can also be selected at each sample point.

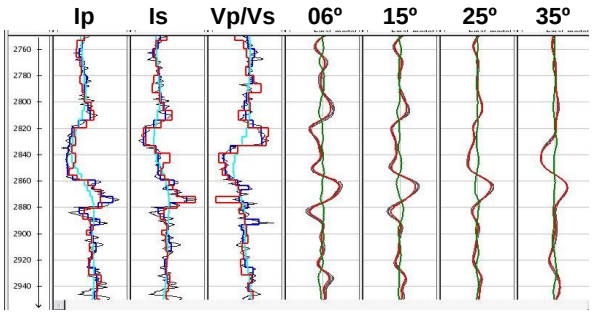

Figure 5: *Inversion QC. For Ip, Is and Vp/Vs ratio the black line is the original well log; cyan, the initial model; blue, the well log upscaled for the stratigraphic grid resolution; and red, the inversion results. With respect to the seismic traces, the black trace is the real seismic trace; red, synthetic trace created from the inversion results; and green, the difference between the real and synthetic trace (residual).*

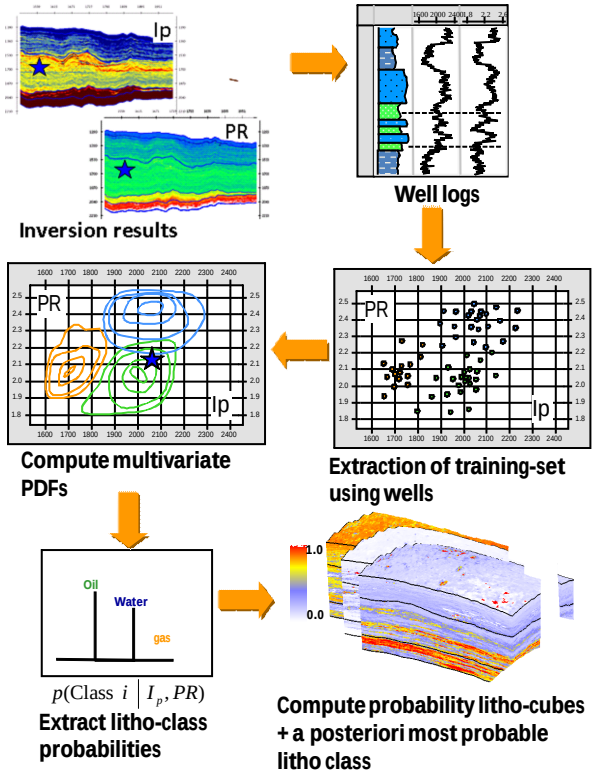

Figure 6: *Workflow for the lithofacies classification.*

Results

Uncertainty assessment was one of the main objectives for geologist to better constrain the geological model in areas with sparse well control, as on the east side of the field. Log scale analysis of the relationship between rock facies and inverted seismic attributes highlights an important lateral variation of acoustic impedance in the reservoir due to variation of the overlying sediment column thickness. Extracting the impedance from the initial (low frequency) model along a key reservoir layer reveals clearly the presence of a large scale E-W impedance trend. This trend is still apparent in the inversion results, as shown in **Figures 7a and 7b**.

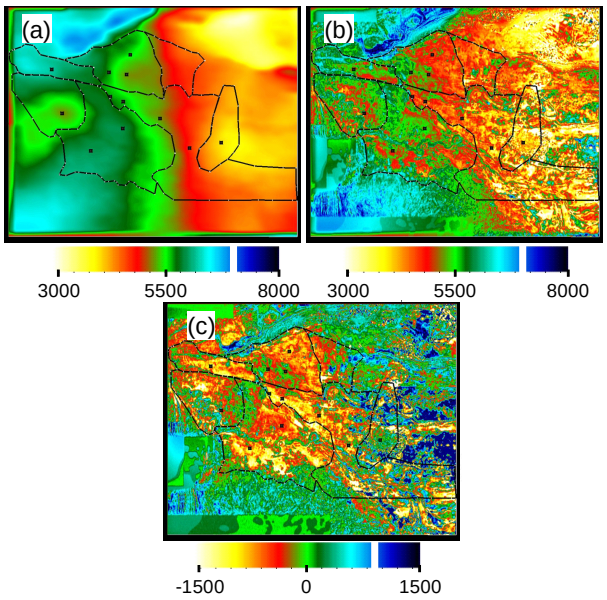

Figure 7: *(a) Initial impedance model extracted along a selected reservoir layer, (b) inversion result, and (c) relative impedance generated for the lithofacies classification.*

Cross-plots of seismic-derived attributes and Bayesian classification tests concluded that the best parameters for discriminating the five lithofacies were relative P-Impedance (R-*Ip*) and *Vp*/*Vs* ratio. The R-*Ip* model was generated by removing the low frequency initial model from the inverted results. **Figure 8** shows the training set and PDF defined for each lithofacies in the R-*Ip Vs Vp*/*Vs* crossplot. The overall classification performance was summarized using a confusion matrix which gives information about the classifier success and mis-classification rates at blind wells used for validation.

In traditional Bayesian classification, a priori facies proportions, *p(c)*, are often assumed constant across the entire field. Defining global facies proportions for this field was not applicable due to the lateral heterogeneity of the sand distribution in different parts of the field. Instead, spatially variable facies proportions were defined based on the different depositional systems and production zones. In each zone (delimitated by black contours on **Figure 9**, a 3-D facies proportion trend was computed from facies log data at key wells. Next, in order to derive realistic lithofacies probability cubes, the following workflow was applied:

- Step 1. Perform supervised Bayesian classification using the same a priori proportion for each lithofacies, i.e., *p(c)*= 0.2 for all five facies. The corresponding lithofacies probability (likelihood) cubes are shown in **Figures 9a** and **9c**.
- Step 2. Perform log analysis of facies distribution of key wells and define a vertically and laterally variable proportion trend in each field zone.
- Step 3. Multiply the facies likelihood cubes obtained in Step 1 with the 3-D facies proportion trends to obtain the a posteriori litho-probability cubes depicted in **Figures 9b** and **9d**.

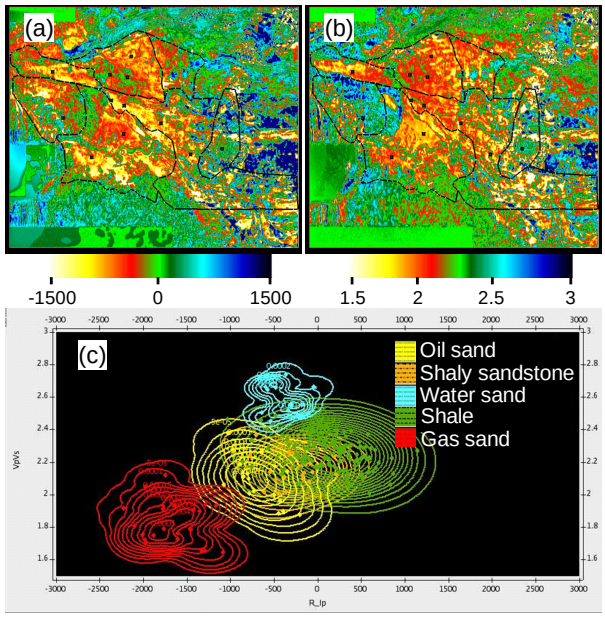

Figure 8: *Attributes used for the classifier. (a) Relative P-Impedance. (b) Vp/Vs Ratio. (c) Bivariate PDFs fitted to each cluster of points.*

Figures 9e and **9f** illustrate the impact of using spatially variable facies proportions instead of global values on the predicted lithofacies distribution. This spatial constraints allowed to better integrate the geological interpretation and capture the lateral heterogeneity of the reservoir. The definition of this lithofacies proportion was tested several times to achieve coherent results. In addition to providing useful information for well planning uncertainty analysis, the seismic-derived litho-probability cubes can easily be integrated as secondary data in reservoir characterization workflows using Sequential Indicator Simulation or Truncated Gaussian Simulation techniques, as for example in Doyen (2007).

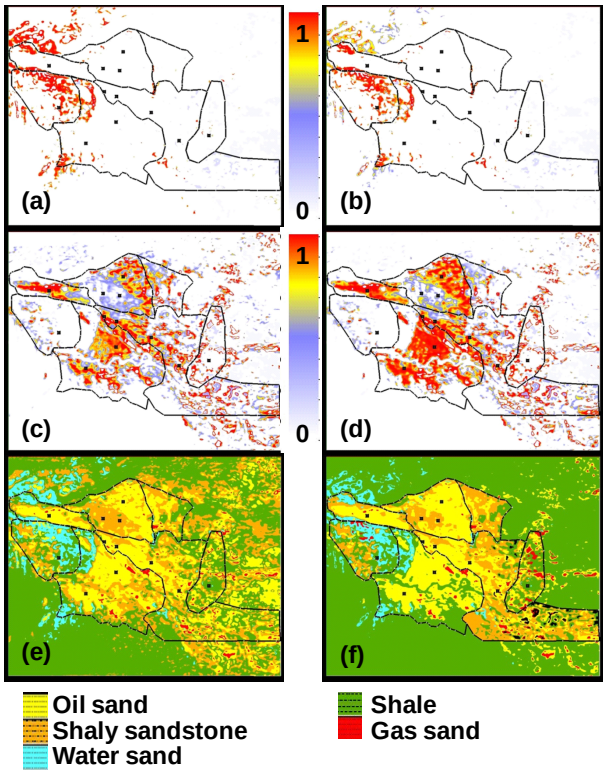

Figure 9: *Lithofacies classification results. Water sand probability using equal (a) and spatially variable (b) facies proportions. Oil sand probability using equal (c) and spatially variable (d) proportions. Most probable lithology using equal (e) and spatially variable (f) proportions.*

Conclusions

A probabilistic approach was applied to derive lithofacies information from inverted seismic attributes and quantify the uncertainty in seismic lithology prediction. Careful data conditioning was critical to the success of the inversion and lithology prediction workflow. Results from the simultaneous elastic inversion, using four sub-angle stacks, gave us a good match with the well response. Lithology classification yields realistic geological features using five classes. The use of 3-D facies proportion cubes, derived independently from the seismic attributes, provided more geologically plausible facies models. It also allowed a better prediction of the producing and non-producing zones and a refining of its limits based on inversion and lithofacies classification results. With these results, the asset team will be able to update its geological model and quantify the uncertainty of facies occurrence for their infill process.

Acknowledges

The authors would like to thank PETROBRAS and CGGVeritas for permission to publish this paper.

References

Deschizeaux , B., Coulon, J-P, Duboz, P., Doyen, P., Lafet, Y., 2006. Stratigraphic Elastic Inversion for Seismic Lithology Discrimination in a Turbiditic Reservoir. Expanded Abstract, SEG Annual Meeting, New Orleans.

Doyen, P., Guidish, T. M., and Buyl, M. H., 1989. Seismic Discrimination of Lithology in Sand/Shale Reservoirs: A Bayesian Approach. Expanded Abstract, SEG Annual Meeting, Dallas.

Doyen, P., 2007. Seismic Reservoir Characterization. EAGE.

Castagna, J. P., Batzle, M. L. and Eastwood, R. L., 1985. Relationships between compressional wave and shear-wave velocities in clastic silicate rocks: Geophysics, 50, 571-581.